Title

Single-molecule observations of neck linker conformational changes in the kinesin motor protein

Journal

Nature Structural & Molecular Biology, 13(10)

ISSN

1545-9985

Authors

Tomishige, M
Stuurman, N
Vale, R

Publication Date

2006-10-01

Peer reviewed

Single molecule observations of the neck linker conformational changes in the kinesin motor protein

Michio Tomishige[1,2], Nico Stuurman[2] & Ronald D. Vale[2]

[1]Department of Applied Physics, The University of Tokyo, 7-3-1 Hongo, Bunkyo-ku, Tokyo 113-8656, Japan

[2]Howard Hughes Medical Institute and Department of Cellular and Molecular Pharmacology, University of California, San Francisco, 600 16th Street, San Francisco, California 94107, USA

Correspondence should be addressed to R.D.V. (vale@cmp.ucsf.edu) or to M.T. (tomishige@ap.t.u-tokyo.ac.jp).

Ron Vale
Department of Cellular and Molecular Pharmacology
University of California, San Francisco
Genentech Hall (Room N312E)
600 16th Street
San Francisco, CA 94107, USA
Phone: 415-476-6380
FAX: 415-476-5233
Email: vale@cmp.ucsf.edu

Kinesin-1 is a dimeric motor protein that moves cargo processively along microtubules. Kinesin motility has been proposed to be driven by the coordinated forward extension of the neck linker (a ~12-amino acid peptide) in one motor domain and the rearward positioning of the neck linker in the partner motor domain. To test this model, we have introduced fluorescent dyes selectively into one subunit of the kinesin dimer and performed "half molecule" fluorescence resonance energy transfer to measure conformational changes of the neck linker. When kinesin binds with both heads to the microtubule, we show that the neck linkers in the rear and forward heads extend forward and backwards respectively. During ATP-driven motility, the neck linkers switch between these conformational states. These results support the notion that neck linker movements accompany the hand-over-hand motion of the two motor domains.

Kinesin-1 (conventional kinesin) is a dimeric motor protein that transports cellular cargoes along microtubules within cells[1,2]. Kinesin-1 (hereafter referred to as kinesin) is a highly processive motor that can take ~150 steps in 8-nm increments along a microtubule before dissociating[3-5]. Structural studies using kinesin monomer have suggested how conformational changes, driven by transitions in the ATPase cycle, generate linear motion of kinesin along a microtubule track. Crystal structures revealed that the compact catalytic core (also termed the "head") is followed by a short 12-amino acid peptide (termed the "neck linker"), which is disordered in some crystal structures[6-8] and ordered and extended along the length of the catalytic core in others[7-11] (**Fig. 1a**, green). A spectroscopic and cryo-electron microscopy (cryo-EM) study performed with truncated kinesin monomers bound to microtubules first revealed that the "docked" state is favored when the catalytic core contains bound ATP, while the "undocked" state predominates in the nucleotide-free and ADP states[12]. These results prompted a model[13] in which the exchange of ATP for ADP in the "leading" head of the microtubule-bound kinesin dimer triggers the docking of the neck linker and a ~16 nm displacement of the "trailing" head upon its to release from the microtubule. After a rapid diffusional search, rebinding of the displaced kinesin head to next available forward tubulin binding site results in a net 8 nm center-of-mass movement of kinesin. The 16 nm-displacement of kinesin heads has recently been measured[14], supporting the hand-over-hand model. Several studies on neck linker conformation also have been interpreted as consistent with this model[15-21]. In addition, an essential role of the neck linker in unidirectional, processive movement has been demonstrated through mutagenesis[22] and crosslinking[23] studies. However, the neck linker conformational state model has been questioned in a kinesin dimer, and alternative models for kinesin processivity have been suggested[24,25].

Because of its small size (~12 amino acids), developing probes for the neck linker conformational change has been challenging. A cryo-EM study examined neck linker position by inserting a relatively large SH3 domain just distal to the neck linker sequence as an EM marker[16]. This study identified SH3 density in-between adjacent motor domains bound along a microtubule protofilament in the presence of AMP-PNP (a very slowly hydrolysable ATP analogue), as expected from the neck linker model. However, the individual neck linkers from the forward and rear heads could not be distinguished, and it was not established whether the insertion of the SH3 into the neck linker altered kinesin processivity (although the ATPase activity was shown to be normal). Using a fluorescence spectroscopy approach, Rosenfeld and colleagues[18,19] found that two tetramethyl rhodamines inserted into both neck linkers of a kinesin dimer demonstrated changes in fluorescence (due to rhodamine dimerization), showing that the neck linkers came close together or moved apart in a nucleotide-dependent manner. Asenjo *et al*.[20,21] took another approach of measuring neck linker orientation/mobility in a kinesin dimer by fluorescence polarization microscopy and again detected nucleotide- and microtubule-dependent changes. Both the Rosenfeld and Asenjo studies supported the neck linker conformational change model for the kinesin dimer and provided further information on how neck linker dynamics are controlled by chemical transitions in the ATPase cycle.

While previous investigations provided valuable information on structural states of kinesin dimer, these studies either involved averaging large number of molecules in population measurements[16,18-21] or investigated single molecules at saturating ATP concentrations where conformational transitions within a chemical cycle could not be discerned[20,21]. In addition,

previous studies introduced probes into both neck linkers of the dimer. However, as the two neck linkers are believed to adopt opposing conformations in a processively moving kinesin dimer[13], it would be advantageous to selectively label a single neck linker within the kinesin dimer. In addition, the measurements should be made at a single molecule level to distinguish these two populations and to detect dynamics in the conformational states of the neck linker. Here, we have introduced donor and acceptor fluorescent dyes selectively into one subunit of the human Kinesin-1 dimer and measured fluorescence resonance energy transfer at the single molecule level. We show that the neck linkers in the rear and forward heads extend forward and backwards respectively when bound to the microtubule in the presence of AMP-PNP, consistent with previous predictions[12,13]. During processive motion at low ATP concentrations, transitions in FRET efficiency are observed, occurring approximately once per 8 nm displacement of the motor. These results support a model in which neck linker movements facilitate the hand-over-hand motion of the two motor domains.

RESULTS

Identifying dye-labeling sites for single molecule FRET

In this study, we used single molecule fluorescence resonance energy transfer (smFRET) to measure conformational states of the neck linker in a microtubule-bound or a processively moving kinesin. We first tested where dyes could be placed in the kinesin dimer without affecting motility (summarized in **Supplementary Fig. 1** online). Various single cysteine substitutions were introduced into a "cysteine-light" kinesin homodimer[12,14,23], the protein was labeled with Cy3 or tetramethyl rhodamine, and the dye-labeled kinesin was tested for processive motility using single molecule, total internal reflection fluorescence (TIRF)

microscopy[23]. Of 20 cysteine positions tested, 6 did not appreciably affect processive motion. Among these were substitutions just past the end of the neck linker (residue 342), and at the plus-end oriented "tip" of the catalytic core (residue 215). A dye pair at residues 215-342 was therefore selected to monitor the position of the neck linker relative to the catalytic core in dimeric kinesin.

Single molecule FRET observations of kinesin monomers

To validate our approach for measuring neck linker position, we first determined whether smFRET could detect the nucleotide-dependent conformational changes in the neck linker of a Cys-light kinesin monomer (K349: residues 1-349 of human ubiquitous kinesin), as previously observed by bulk solution FRET[12]. To monitor the position of the neck linker, Cy3 (donor dye) and Cy5 (acceptor dye) were covalently linked to cysteines introduced just past the end of the neck linker (in case of monomers, we used residue 347 so as to amplify the nucleotide-dependent FRET efficiency changes) and either at the plus-end-oriented "tip" of the catalytic core (residue 215) or the minus-end-oriented "base" of the core (residue 43) (**Fig. 1a,b**). Although the Cy3 and Cy5 maleimide-modified dyes could not be directed to particular cysteines, we could selectively observe individual kinesins that were dual labeled with each dye (**Fig. 1c**). Cy3 and Cy5 were excited sequentially by laser total internal reflection illumination, and the Cy3 and Cy5 (or FRET) emissions were imaged simultaneously by spatially separating the two emission wavelengths onto the faceplate of a cooled intensified CCD camera (**Fig. 1c** and Methods). We assured that single molecules were recorded, since single photobleaching events of either the Cy3 or Cy5 dye were observed, which resulted in an abrupt loss of the FRET signal (**Supplementary Video 1** online).

We found that the 215-347 dye pair showed greater average smFRET efficiency in the presence of AMP-PNP when compared with nucleotide-free conditions, while the opposite result was obtained with the 43-347 dye pair (**Fig. 1d**; histograms are shown in **Supplementary Fig. 2** online). In fact, nucleotide-dependent differences in FRET efficiencies were greater in this study compared with those obtained by the bulk measurements[12], partly due to the differences in the dyes or their positions, and also possibly because singly-labeled, non-microtubule-bound, or inactive motors can be excluded using single molecule measurements. As a control, two dyes were placed within the catalytic core itself (28-149), and no nucleotide-dependent change in smFRET efficiency was observed (**Fig. 1d**). Rice *et al*.[12] also identified two ATP hydrolysis mutants in the switch II region of the nucleotide active site, one of which (E236A) stabilizes the neck linker in the ATP-like, docked conformation while the other (G234A) favors the nucleotide-free-like, detached conformation. In the presence of 1 mM ATP, we found that the 215-347 dye pair showed a greater smFRET signal in the E236A mutant compared with the G234A mutant, while the converse result was obtained with the 43-347 dye pair (**Fig. 1d**). Thus, smFRET generally reveals similar neck linker positions for microtubule-bound kinesin monomers with different nucleotides and mutations to that reported previously for bulk population FRET measurements and cryo-EM[12].

To model the neck linker structure in monomer, we estimated the distances between donor/acceptor dyes using the median values of the smFRET efficiencies (see the legend of **Fig. 1d** and Methods). We acknowledge, however, that these distance estimations are unlikely to be precise because of uncertainties in dye orientation (assumed in our calculations to be

random) and dye location due to the positioning of the chemical linker (which separates the dye center and the cysteine by ~1.5 nm). Nevertheless, the estimated distances in the presence of AMP-PNP are in good agreement with those observed in the neck linker docked crystal structure[9] (**Fig. 1b**, left). However, the estimated distances in the nucleotide-free condition differ from what might be expected for a totally disordered neck linker (if the disordered neck linker behaves as an entropic spring, it would be positioned near the base of the neck linker on the core, producing a higher FRET efficiency (~60%) for the 215-347 dye pair). The slight inconsistency might be due to a preferred dye orientation, which would affect the κ^2 value in the Förster distance calculation between the dye pair (see Methods). Alternatively, the neck linker may adopt "backwards-extending" configuration[26] (**Fig. 1b**, right) in the nucleotide-free state.

Static FRET of microtubule-bound kinesin dimers

We next examined the neck linker positions in a kinesin dimer bound with both heads to a microtubule in the presence of AMP-PNP[27] by selectively introducing FRET reporters into one of the two neck linkers (**Fig. 2a**). To accomplish this, we introduced a cysteine pair (215-342) into a cysteine-light kinesin gene (K490; residues 1-490) bearing a Strep-tag[28] and co-expressed it with a cysteine-light K490 with a His_6-tag, and then purified the heterodimer by two-step affinity chromatography (see Methods). Cy3/Cy5 labeled heterodimers showed processive movement (average velocity at 1 mM ATP was 450 ± 150 nm/s (n = 30), which is similar to that for non-mutant truncated human kinesin fused to GFP[29]; **Supplementary Video 2** online). This result indicates that mutation and dye-labeling on these sites in the heterodimer did not alter the motor activity (consistent with our previous work on dye labeled homodimers;

Supplementary Fig. 1 online). SmFRET efficiencies from this 215-342 labeled, microtubule-bound heterodimer showed a bimodal distribution of low and high FRET efficiencies in the presence of AMP-PNP (**Fig. 2b**). This result is consistent with the neck linker model in which the 215-342 dye pair in the leading head would exhibit low FRET efficiency (~30% for ~6 nm separation) (its neck linker pointing backwards; **Fig. 2a**, left), while the same dye pair in the trailing head would display high FRET efficiency (~100% for ~2 nm separation) (**Fig. 2a**, right)[13,26].

In the above heterodimer experiment, the 215-342 dye labeled head occupied the leading or trailing position with equal probability. To eliminate this heterogeneity and further test the neck linker model, we performed smFRET measurements with a kinesin heterodimer in which one polypeptide chain contained the G234A mutation while the other contained the E236A mutation. In this heterodimer in the presence of ATP, the E236A-containing head would be predicted to be in the rear (since its neck linker is locked in for forward-pointing, docked conformation), while the G234A-containing head would be leading (its neck linker detached and pointing backwards) (**Fig. 1d**). When the 215-342 dye pair was introduced into the G234A chain of the G234A:E236A heterodimer, the major peak in FRET efficiency histogram was observed at ~0.4 for microtubule-bound heterodimers in the presence of 1 mM ATP (**Fig. 2c**, upper), although there was a trailing distribution with higher FRET suggesting perhaps some additional conformational states of the motor. In contrast, when the same 215-342 fluorescent dye pair was introduced into the E236A chain of the same heterodimer, the major peak in the single molecule histogram was observed at ~0.8 FRET efficiency (**Fig. 2c**, lower). These histograms differ from the bimodal distribution of the 215-342 dye pair in the kinesin

without these switch II mutations (**Fig. 2b**), indicating that the neck linkers in leading and trailing heads adopt different configurations.

We also wished to determine the positioning of the mutant heads in the heterodimer by substituting a cysteine in the 215 position of the E236A chain and a cysteine in the 43 position of the G234A chain (**Fig. 2d**, left). This arrangement gave rise to high FRET efficiency for microtubule-bound heterodimers in the presence of ATP (**Fig. 2e**, upper), although the distribution was broad due to noise or perhaps other motor states (e.g. one-head bound states). In contrast, low FRET efficiency was observed with the opposite pairing (215 cysteine on the G234A chain and the 43 cysteine on the E236A chain: **Fig. 2d**, right) (**Fig. 2e**, lower). Thus, the FRET efficiency depended upon dye positioning in the two mutant chains. Taken together with the experiments in **Figure 2c**, these data indicate that the E236A chain assumes the position of the trailing head and has its neck linker extending forward, while the G234A chain is the leading head and has its neck linker pointing backwards. This heterodimer position likely reflects an intermediate in the kinesin motility cycle in which the rear and forward heads are in the ATP and nucleotide-free (or ADP) states respectively (**Fig. 2a**).

Dynamic FRET of processively moving kinesin dimers

We next wished to determine whether the neck linker changes its conformation when the leading and trailing heads exchange their positions in an active kinesin dimer moving processively along a microtubule. Since our acquisition rate was ~60 images/sec (see the legend of **Fig. 3a**), our temporal resolution was insufficient to observe any transient conformations during the kinesin step itself (10 msec or less)[17,18,30], but we could hope to

observe the conformation(s) of the kinesin neck linker during the dwell times between steps. To prolong these dwell times, we slowed down kinesin motility by reducing the ATP concentration (~1 μM) so that ATP binding becomes rate limiting in the cycle. With the neck linker FRET reporter pair (215-342 in one head of a heterodimer), anti-correlated increases and decreases in Cy3 and Cy5 fluorescence were observed and the calculated FRET efficiency showed transitions between high and low FRET states (**Fig. 3a**; also see **Supplementary Fig. 3** and **Supplementary Videos 3** and **4** online). We simultaneously tracked the centroid of the spots and confirmed that these molecules moved processively along axonemes (**Fig. 3a**, purple), although our spatial resolution was lower compared with other higher spatial, lower temporal resolution methods[14]. In some cases, we were able to track the centroid of moving 215-342 heterodimer kinesin molecules for several seconds before one of the dyes photobleached. In these cases (n = 22 molecules), we could estimate the number of anti-correlated transitions in FRET efficiency (120 in total) and the distance traveled (1.25 μm in total) during a particular time period, which equates to a 10.4 nm displacement per FRET transition (**Fig. 3b**). This calculated step size does not agree precisely with the known 8.3 nm kinesin step size[3], but this is not surprising given that transitions with short dwell times could not be detected due to the limited temporal resolution of our system (see **Supplementary Fig. 4** online). We also measured the dwell times between transitions, which could be fit reasonably well to exponential distributions (**Supplementary Fig. 4** online). The average dwell times in the high and low FRET states were 0.34 ± 0.25 sec and 0.58 ± 0.48 sec respectively, which are similar to the expected dwell time of 0.45 sec (based upon an average motor velocity of 18.5 ± 9.4 nm/s at 1 μM ATP (n = 23)). In summary, these data support the conclusion that anti-correlated changes in Cy3-Cy5 fluorescence are due to conformational changes of the neck linker associated with

ATP-driven kinesin stepping.

To validate that the observed anti-correlated intensity changes represent distance changes between two fluorophores, we introduced a FRET pair at residues 43 and 215 within one catalytic core of a heterodimer; the distance between these residues is not expected to change substantially during motility[7,8]. With the 43-215 pair, anti-correlated Cy3-Cy5 fluorescence changes (>0.2 FRET efficiency change) were not observed during processive movement in the presence of 1 μM ATP (**Fig. 3c** and **Supplementary Fig. 5** online). We also introduced a FRET pair into the base of the neck coiled-coil (Cys342 in both chains), and again found that FRET efficiency was constant during motility (**Fig. 3d** and **Supplementary Fig. 5** online). This result also indicates that the base of the coiled-coil does not unwind extensively (> 3 nm)[23], at least with the temporal inspection available in this study. In addition, using saturating ATP concentrations (1 mM) for the 215-342 heterodimer kinesin, few anti-correlated changes in Cy3-Cy5 fluorescence were observed, as would be expected when the dwell time between steps decreases below our temporal resolution (**Supplementary Fig. 5** and **Supplementary Video 2** online). Fluctuations in intensity of a single dye are common, but in these cases, FRET efficiency changes do not exceed 0.2 and are not accompanied by anti-correlated changes in the second dye, as observed clearly for the dynamic neck linker FRET.

DISCUSSION

In this study, we explored conformational states of the neck linker, a proposed mechanical element for motility, in kinesin dimers using single molecule FRET. Previous studies by Rice *et al.*[12] reported a nucleotide- and microtubule-dependent docking/undocking conformational

change of the neck linker with the catalytic core in kinesin monomers. Fluorescence reporters[18-21] or markers for electron microscopy[16] placed in kinesin dimers have yielded results that are generally consistent with prior monomer studies. Specifically, these kinesin dimer studies have shown that non-hydrolyzable ATP analogues cause the neck linker to adopt a well-ordered forward docked state, whereas the neck linker becomes more flexible in the absence of nucleotide. However, information on the neck linker conformations in the leading and trailing heads has been lacking, as has evidence for alternating structural changes in the neck linkers during hand-over-hand movement. Here, we provide evidence that the neck linkers in the leading and trailing heads adopt different conformations and that individual neck linkers switch between leading and trailing conformations during ATP-driven processive motion (**Fig. 4**). These notions are consistent with a previous model for kinesin processive motility[13] in which ATP-dependent docking of the neck linker in the leading head moves the partner head forward to facilitate its binding to the forward tubulin site.

Dynamic measurements of nucleotide-dependent conformational changes in myosin's "lever arm" position have been made by FRET[31,32] and at the single molecule level by fluorescence polarization[33]. However, the small size of kinesin's neck linker (~12 a.a.) compared with myosin's mechanical element (~130 a.a. converter domain and lever arm helix)[34] poses special challenges for measurements of its conformational changes. For example, many of cysteine substitutions followed by fluorescent dye labeling resulted in either partial or complete inactivation of processive motion (**Supplementary Fig. 1** online). Even labeling of some cysteines (e.g. residues 220, 333) that preserved activity of monomer in prior studies[12] did not yield fully active processive dimers. A likely explanation is that such introduced fluorescent

dyes might interfere with head-head interactions or coordination in the kinesin dimer. Thus, successful execution of this work involved testing various positions of dual dye labeling for ones that allowed normal movement. In addition, measurements of neck linker conformational changes required introducing probes into only one of the two subunits of the kinesin dimers, so as not to generate complex signals from dyes attached to different combinations of the four possible cysteine residues in a homodimer. In this study, selective labeling of one kinesin subunit was achieved by introducing C-terminal protein tags that allowed selective affinity purification of kinesin heterodimers with one Cys-light subunit and one subunit with two introduced cysteines for dye labeling (or with active site mutations, as was the case with experiments employing the G234A:E236A heterodimer).

We detected the neck linker positions in a microtubule-bound kinesin dimer by introducing FRET probes selectively into one of the two neck linkers. FRET efficiencies from microtubule-bound kinesin dimer showed two distinct populations with nearly equal probability corresponding approximately to the AMP-PNP and nucleotide-free states observed in the monomer. However, the conformations in the leading and trailing heads could not be distinguished from this experiment. To distinguish the two neck linkers in leading and trailing heads, a G234A:E236A mutant heterodimer proved valuable. Consistent with our expectation from the neck linker model, the G234A head was highly probable in the leading position and the E236A head in the trailing position. Using this heterodimer, we also provide the first evidence for the neck linker conformational states in this two-head-bound state: the neck linker is pointing forward in the trailing head (ATP-like state (E236A)) and pointing backwards in the leading head (nucleotide-free state (G234A)). The forward-extending neck linker in the

trailing head is likely to reflect the state observed in crystal structures where the neck linker is docked onto the catalytic core[7-11]. However, the precise conformation of the backwards-pointing neck linker remains uncertain. One possibility is that this neck linker is highly mobile, constrained to pointing rearward by a connection to the rear head via the coiled-coil domain; measurements that assess neck linker flexibility support this view[12,15,16,21]. A second possibility is that the backwards-pointing neck linker also is "docked" to a specific site on the catalytic core[26], as has been observed for a related kinesin (Kinesin-5 (Eg5))[35]. Such a backwards-docked conformation might facilitate ADP release when the detached head rebinds to a forward tubulin-binding site[20,36]. Our measurements of FRET efficiency with nucleotide-free kinesin monomers also can be interpreted in favor of a backwards-docked state, although caveats exist (e.g. effects of dye labeling on protein conformation and uncertainties in dye orientation for FRET distance calculations). The existence of a nucleotide-free "docked state" therefore merits further investigation using different probes.

In this study, we also observed FRET efficiency changes of a dye pair in a single neck linker within a kinesin dimer during slow processive movement under low ATP concentrations. On average, these transitions took place approximately once per 8 nm step, although we lacked sufficient spatiotemporal resolution to show that FRET transitions occurred simultaneous with an 8 nm step. Nonetheless, our results provide the first direct evidence for the alternating neck linker conformational changes during processive movement.

The dynamic FRET measurements also provide some insight into the "waiting" state of kinesin at low ATP concentrations, which has been subject to various interpretations (reviewed in

Carter and Cross[25]). One model proposes that kinesin waits for the next ATP as a one-head bound intermediate, in which one head is bound tightly to the microtubule (nucleotide-free "waiting" head) while the ADP-bound partner head is detached and potentially poised in a position for the next forward step[4,30]. However, recent kinetic and fluorescence polarization data suggest that the ADP-bound head also may be tethered to the microtubule, but incapable of rapidly releasing ADP, perhaps because of the forward neck linker position in this two-head bound intermediate[20,37]. Our results show a single neck linker in a kinesin molecules alternates between two FRET states during processive motion, which is most consistent with a two-head bound intermediate state. If the kinesin moved in an inchworm manner[38] or with a consistent one-head bound intermediate state (with two mobile neck linkers in the nucleotide-free and ADP-bound head), then less obvious FRET transitions would be expected. However, alternate FRET transitions might be observed with a one-head bound intermediate, if the neck linker on the waiting head adopts a backwards-pointing structure as discussed before (FRET efficiency would then represent transitions between an ordered, nucleotide-free and a disordered, ADP-bound states). In addition, it is possible that the two models may not be absolute, as two-head bound and one-head bound conformations may both occur for kinesin molecules moving at low ATP conformation. The question of whether kinesin waits with one-head or two-heads bound (or both) will require measuring the spacing between the heads during motility. Single molecule FRET measurements of head-head positioning with improved temporal resolution will provide a powerful tool for such investigations.

In conclusion, single molecule FRET reporters provide evidence for distinct conformations of the neck linkers in a kinesin dimer. In a static two-head-bound kinesin dimer, we show that

the neck linkers extend forward and backwards in the trailing and leading heads respectively, and that these conformational states alternate during ATP-driven processive motility. This data, in conjunction with previous FIONA measurements[14] and other studies showing alternation in kinesin stepping behavior[39-41], support models in which the neck linker movements facilitate the hand-over-hand stepping of the kinesin heads during processive motility (**Fig. 4**).

Methods

DNA cloning. Cysteines (K28C, S43C, S149C, E215C, K342C, E347C) and/or mutations in switch II region (E236A, G234A) were introduced into a "cysteine-light" human ubiquitous kinesin 349-amino acid[12] monomer or a 490-amino acid dimer, each containing a C-terminal His_6 tag. For heterodimers, a coexpression vector was constructed that carries two 490-amino acid kinesin sequences in tandem: the first kinesin sequence contained a C-terminal Strep-tag (9-amino acid: AWRHPQFGG)[28] and the second was followed by a His_6-tag. Each kinesin gene has its own ribosome-binding site, and two genes are flanked by a T7 promoter and a T7 terminator. All constructs were verified by DNA sequencing.

Protein purification. Monomeric kinesins were expressed and purified as described[23]. Heterodimeric kinesins were expressed, lysed and then purified by Ni-NTA chromatography as described[23]. Heterodimers were further purified by Strep-Tactin (streptavidin mutant) affinity purification[28]. Elution from Ni-NTA resin was loaded on Strep-Tactin Sepharose (IBA GmbH) column, and then washed with ST-buffer (50 mM phosphate buffer [pH 7.0], 250 mM NaCl, 2 mM $MgCl_2$, 10 mM 2-mercaptoethanol, 100 μM ATP). Heterodimers were eluted with ST buffer containing 2.5 mM D-desthiobiotin. Purified monomeric and heterodimeric kinesins were dialysed against 25 mM Pipes [pH 7.0], 100 mM NaCl, 1 mM EGTA, 2 mM $MgCl_2$, 50 μM ATP for 4 hr at 4°C. Protein concentrations were determined by Bradford assay using BSA as a standard. Typical yields of heterodimer proteins were 0.2-0.5 mg from 1 L of bacterial culture. Dialysed kinesin was reacted with Cy3-maleimide and Cy5-maleimide (Amersham Biosciences) at a molar ratio of 1:10:10 for motor head:Cy3 dye:Cy5 dye, for 4 hr at 4°C. Unreacted dyes were quenched with 1 mM DTT and then removed through

microtubule affinity purification as described[23], except that 100 μM ATP was used for releasing motors from microtubules.

Single molecule fluorescence microscopy. Single molecule FRET microscopy was based on a custom-built total internal reflection fluorescence microscope as described previously[23,29]. Dye-labeled heterodimeric kinesins were attached onto the axonemes (purified from sea urchin sperm flagella) in the presence of 1 mM AMP-PNP or 5 U ml^{-1} apyrase, or moved along axonemes in the presence of ATP and an ATP regenerating system as described previously[29]. The dye-labeled monomers were bound to axonemes at a density where single fluorescent molecules could be clearly distinguished. Cy3 and Cy5 dyes were illuminated with an argon laser (514 nm) and a He-Ne laser (632 nm), respectively (10-20 mW laser power). The fluorescence images from Cy3 and Cy5 (or FRET) were separated using Dual-View (Optical Insights) and then projected side-by-side on a cooled, intensified CCD camera (XR/MEGA10-Z, Stanford Photonics, Inc.) or an intensified CCD camera (XR/MEGA10, Stanford Photonics, Inc.) (acquisition rate: 60 frames per sec). For the static FRET measurements, both Cy3 and Cy5 fluorophores were directly illuminated by sequential excitation with the argon and He-Ne lasers. Both lasers were used to identify molecules that exhibited little or no FRET (i.e. molecules labeled with both Cy3 and Cy5, but which did not emit in the Cy5 channel after excitation of Cy3). For the dynamic FRET measurements, alternate laser excitation was not possible to retain sufficient temporal information on the FRET signal, and instead images were taken by excitation with the argon laser.

Data analysis. Images for static FRET efficiencies were analyzed using Image J

(http://rsb.info.nih.gov/ij/) with custom-designed plug-in software. Images for donor or acceptor excitations were averaged over ~120 frames. This set of images was used to identify Cy3/Cy5 dual labeled motors and its Cy3 and Cy5 fluorescence intensities. Axonemes that were sparsely coated with fluorescence spots (less than 1 spot per 2 μm microtubule (~35 pixels)) were used for data analysis to reduce the chance that two distinct Cy3 and Cy5 spots happened to co-localize on the axonemes within one pixel (57 nm). FRET efficiencies were calculated as $E = 1/[1 + I_D/\{(I_A - \chi I_D)\cdot\gamma\}]$, where I_D and I_A are background subtracted intensities from the donor and acceptor channels, respectively, χ is the crosstalk of donor intensity into acceptor channel, and γ is a parameter to correct for different detection efficiencies of the two channels and the quantum yields of donor/acceptor dyes. χ was determined experimentally by observing donor only labeled motors, and γ was determined by observing the donor/acceptor intensity changes after photobleach of the acceptor dye for the motors showing ~100% FRET (342:342 mutant; **Supplementary Video 1** online). Cy5 intensities corrected as $(I_A - \chi I_D)\cdot\gamma$ are shown in figures for time traces. The distances r between donor and acceptor dyes were estimated using the relationship: $E = [1 + (r/R_0)^6]^{-1}$, where $R_0 = 5.3$ nm was used as the Förster radius (assuming a constant orientation factor κ^2 of 2/3)[42]. Images for dynamic FRET measurements were averaged over 4 frames and then analysed using custom-designed MATLAB (The MathWorks) software. Background subtracted fluorescence intensities from the donor and acceptor channels were determined for each frames and the corrected FRET efficiencies were determined as described above. Centroids of the fluorescence spots were tracked using cross-correlation algorithm[43]. Fluorescence spots that did not show clear unidirectional movement (motor was inactive or its displacement was small compared to the noise) were not subjected to further data analysis. Analysis also were only performed on spots

that showed decent signal-to-noise ratio in fluorescence intensities, minimal blinking, slow movement (<40 nm s^{-1}), and long duration before photobleaching or detachment from the microtubule. To identify anti-correlated transitions, we first applied a 7-frame running average filter to the FRET efficiency traces to reduce the noise and then identified transitions that accompany with large FRET efficiency changes (more than 0.3).

References

1. Vale, R.D. The molecular motor toolbox for intracellular transport. *Cell* **112**, 467-480 (2003).
2. Hirokawa, N. & Takemura, R. Molecular motors and mechanisms of directional transport in neurons. *Nat. Rev. Neurosci.* **6**, 201-214 (2005).
3. Svoboda, K., Schmidt, C.F., Schnapp, B.J. & Block, S.M. Direct observation of kinesin stepping by optical trapping interferometry. *Nature* **365**, 721-727 (1993).
4. Hackney, D.D. Evidence for alternating head catalysis by kinesin during microtubule-stimulated ATP hydrolysis. *Proc. Natl. Acad. Sci. USA* **91**, 6865-6869 (1994).
5. Vale, R.D. *et al*. Direct observation of single kinesin molecules moving along microtubules. *Nature* **380**, 451-453 (1996).
6. Kull, F.J., Sablin, E.P., Lau, R., Fletterick, R.J. & Vale, R.D. Crystal structure of the kinesin motor domain reveals a structural similarity to myosin. *Nature* **380**, 550-555 (1996).
7. Kikkawa, M. *et al*. Switch-based mechanism of kinesin motors. *Nature* **411**, 439-445 (2001).
8. Nitta, R., Kikkawa, M., Okada, Y. & Hirokawa, N. KIF1A alternatively use two loops to bind microtubules. *Science* **305**, 678-683 (2004)
9. Sack, S. *et al*. X-ray structure of motor and neck domains from rat brain kinesin. *Biochemistry* **36**, 16155-16165 (1997).
10. Kozielski, F. *et al*. The crystal structure of dimeric kinesin and implications for microtubule-dependent motility. *Cell* **91**, 985-994 (1997).
11. Sindelar, C.V. *et al*. Two conformations in the human kinesin power stroke defined by X-ray crystallography and EPR spectroscopy. *Nat. Struct. Biol*. **9**, 844-848 (2002).
12. Rice, S. *et al*. A structural change in the kinesin motor protein that drives motility. *Nature*

402, 778-784 (1999).

13. Vale, R.D. & Milligan, R.A. The way things move: looking under the hood of molecular motor proteins. *Science* **288**, 88-95 (2000).
14. Yildiz, A., Tomishige, M., Vale, R.D. & Selvin, P.R. Kinesin walks hand-over-hand. *Science* **303**, 676-678 (2004).
15. Rice, S. *et al*. Thermodynamic properties of the kinesin neck-region docking to the catalytic core. *Biophys. J.* **84**, 1844-1854 (2003).
16. Skiniotis, G. *et al*. Nucleotide-induced conformations in the neck region of dimeric kinesin. *EMBO J.* **22**, 1518-1528 (2003).
17. Rosenfeld, S.S., Jefferson, G.M. & King, P.H. ATP reorients the neck linker of kinesin in two sequential steps. *J. Biol. Chem*. **276**, 40167-40174 (2001).
18. Rosenfeld, S.S., Xing, J., Jefferson, G.M., Cheung, H.C. & King, P.H. Measuring kinesin's first step. *J. Biol. Chem*. **277**, 36731-36739 (2002).
19. Rosenfeld, S.S., Fordyce, P.M., Jefferson, G.M., King, P.H. & Block, S.M. Stepping and stretching: how kinesin uses internal strain to walk processively. *J. Biol. Chem*. **278**, 18550-18556 (2003).
20. Asenjo, A.B., Krohn, N. & Sosa, H. Configuration of the two kinesin motor domains during ATP hydrolysis. *Nat. Struct. Biol*. **10**, 836-842 (2003).
21. Asenjo, A.B., Weinberg, Y. & Sosa, H. Nucleotide binding and hydrolysis induces a disorder-order transition in the kinesin neck-linker region. *Nat. Struct. Mol. Biol*. **13**, 648-654 (2006).
22. Case, R.B., Rice, S., Hart, C.L., Ly, B. & Vale, R.D. Role of the kinesin neck linker and catalytic core in microtubule-based motility. *Curr. Biol*. **10**, 157-160 (2000).

23. Tomishige, M. & Vale, R.D. Controlling kinesin by reversible disulfide cross-linking: identifying the motility-producing conformational change. *J. Cell Biol*. **151**, 1081-1092 (2000).

24. Schief, W.R. & Howard, J. Conformational changes during kinesin motility. *Curr. Opin. Cell Biol.* **13**, 19-28 (2001).

25. Carter, N.J. & Cross, R.A. Kinesin's moonwalk. *Curr. Opin. Cell Biol*. **18**, 1-7 (2006)

26. Sablin, E.P. & Fletterick, R.J. Coordination between motor domains in processive kinesins. *J. Biol. Chem*. **279**, 15707-15710 (2004).

27. Kawaguchi, K. & Ishiwata, S. Nucleotide-dependent single- to double-headed binding of kinesin. *Science* **291**, 667-669 (2001).

28. Skerra, A. & Schmidt, T.G.M. Applications of a peptide ligand for streptavidin: the Strep-tag. *Biomol. Eng*. **16**, 79-86 (1999).

29. Tomishige, M., Klopfenstein, D.R. & Vale, R.D. Conversion of Unc104/KIF1A kinesin into a processive motor after dimerization. *Science* **297**, 2263-2267 (2002).

30. Carter, N.J. & Cross, R.A. Mechanics of the kinesin step. *Nature* **435**, 308-312 (2005)

31. Suzuki, Y., Yasunaga, T., Ohkura, R., Wakabayashi, T. & Sutoh K. Swing of the lever arm of a myosin motor at the isomerization and phosphate-release steps. *Nature* **396**, 380-383 (1998).

32. Shih, W.M., Gryczynski, Z., Lakowicz, J.R. & Spudich, J.A. A FRET-based sensor reveals large ATP hydrolysis-induced conformational changes and three distinct states of the molecular motor myosin. *Cell* **102**, 683-694 (2000).

33. Forkey, J.N., Quinlan, M.E., Shaw, M.A., Corrie, J.E. & Goldman, Y.E. Three-dimensional structural dynamics of myosin V by single-molecule fluorescence polarization. *Nature* **422**,

399-404 (2003).

34. Houdusse, A., Kalabokis, V.N., Himmel, D., Szent-Györgyi, A.G. & Cohen, C. Atomic structure of scallop myosin subfragment S1 complexed with MgADP: a novel conformation of the myosin head. *Cell* **97**, 459-470 (1999).

35. Turner, J. *et al*. Crystal structure of the mitotic spindle kinesin Eg5 reveals a novel conformation of the neck-linker. *J. Biol. Chem*. **276**, 25496-25502 (2001).

36. Kinosita, K. Jr. *et al*. How two-foot molecular motors may walk. *Adv. Exp. Med. Biol.* **565**, 205-219 (2005).

37. Hackney, D.D. The tethered motor domain of a kinesin-microtubule complex catalyzes reversible synthesis of bound ATP. *Proc. Natl. Acad. Sci. USA* **102**, 18338-18343 (2005).

38. Hua, W., Chung, J. & Gelles, J. Distinguishing inchworm and hand-over-hand processive kinesin movement by neck rotation measurements. *Science* **295**, 844-848 (2002).

39. Asbury, C.L., Fehr, A.N. & Block, S.M. Kinesin moves by an asymmetric hand-over-hand mechanism. *Science* **302**, 2130-2134 (2003).

40. Kaseda, K., Higuchi, H. & Hirose, K. Alternate fast and slow stepping of a heterodimeric kinesin molecule. *Nat. Cell Biol*. **5**, 1079-1082 (2003).

41. Higuchi, H., Bronner, C.E., Park, H.-W., & Endow, S.A. Rapid double 8-nm steps by a kinesin mutant. *EMBO J*. **23**, 2993-2999 (2004).

42. Ishii, Y., Yoshida, T., Funatsu, T., Wazawa, T. & Yanagida, T. Fluorescence resonance energy transfer between single fluorophores attached to a coiled-coil protein in aqueous solution. *Chem. Phys.* **247**, 163-173 (1999).

43. Gelles, J., Schnapp, B.J. & Sheetz, M.P. Tracking kinesin-driven movements with nanometre-scale precision. *Nature* **331**, 450-453 (1988).

Note : Supplementary information is available on the Nature Structural & Molecular Biology website.

ACKNOWLEDGEMENTS

We thank K. Thorn for development of the initial version of the microscope system and for discussions, and U. Wiedemann for support in cloning and protein purification. M.T. is supported by grants from the Mitsubishi Foundation, Asahi Glass Foundation, the Sumitomo Foundation and the Inamori Foundation, and by Grants-in-Aid for Scientific Research on Priority Areas. R.D.V. is supported by grants from the Howard Hughes Medical Institute and the US National Institutes of Health.

AUTHOR CONTRIBUTIONS

M.T. and R.D.V. conceived and designed the experiments. M.T. performed the experiments and data analysis. N.S. contributed to microscope construction and programming. R.D.V. and M.T. discussed the results and wrote the manuscript.

COMPETING INTERESTS STATEMENT

The authors declare that they have no competing financial interests.

Figure Legends

Figure 1 Single molecule FRET measurements of monomeric kinesin. (**a**) Cysteine positions introduced into the Cys-light kinesin for labeling with thiol-reactive dyes (colored in red on the crystal structure of rat kinesin monomer (PDB #2KIN[9]; numbered as in human kinesin)). The neck linker and the neck coiled-coil are shown in green and blue, respectively, and ADP is shown as space filling in cyan. (**b**) Schematics showing neck linker in docked and undocked states (modeled in the later case) of a kinesin monomer bound to a microtubule protofilament (#1TUB). To probe the neck linker conformation, FRET efficiencies between donor and acceptor fluorophores attached to the neck coiled-coil (347) and the catalytic core (43, 149 or 215) were observed. Schematic figures were made with PyMol. (**c**) Images of Cy3 (donor) and/or Cy5 (acceptor) labeled kinesin monomers (43-347 cysteines) bound to an axoneme in the presence of AMP-PNP. Two sets of images were acquired after excitation at 514 and 632 nm (excitation wave lengths of Cy3 and Cy5, respectively), and Cy3 and Cy5 emissions were recorded simultaneously on an intensified CCD camera. Red arrows indicate single molecules labeled with both Cy3 and Cy5 and exhibiting FRET, and white arrows indicate molecules with only Cy3 or Cy5. (**d**) Median ± s.d. values of FRET efficiencies between dye position pair on monomer bound to the axonemes, in the presence of 1 mM AMP-PNP (ATP-like state), 5 U/ml apyrase (nucleotide-free state), and 1 mM ATP with either the E236A mutation or with G234A mutation (see **Supplementary Fig. 2** online for histograms). Numbers of molecules analyzed are shown in parentheses. The AMP-PNP states (1 mM) of the E236A (FRET efficiency of 0.72 ± 0.12; n=10) and G234A (0.45 ± 0.17; n=13) mutants for the 215-347 dye pair were similar to those shown for 1 mM ATP, as expected for these non-hydrolyzing mutants. The

means of the 215-347 and 43-347 FRET pairs are statistically different between the AMP-PNP and apyrase states (P value < 0.001 by Kolmogorov-Smirnov test), whereas the 149-347 and 28-149 dye pairs do not show a significant FRET change between these two nucleotide states (P value > 0.3). These median values are used to calculate estimated distances between dyes (see Methods). In the presence of AMP-PNP, estimated distances for 215-347, 43-347, 149-347 dye pairs are 4.3, 5.6, 5.3 nm, respectively, which are good approximations to the actual distances between Cα atoms of cysteine residues in the rat kinesin crystal structure (shown in **b**, left). In the presence of apyrase, estimated distances for 215-347, 43-347, 149-347 dye pairs are 6.2, 4.7, 5.4 nm (**b**, right).

Figure 2 Neck linker positions in microtubule-bound dimeric kinesin in the two-head-bound intermediate. (**a**) Schematics of two-head-bound intermediate state of kinesin dimer bound to the microtubule, based upon a model[13] predicting that the neck linker in the leading head is pointing rearward (left; similar to the configuration in **Fig. 1b**, right) and the neck linker in the trailing head is docked onto the catalytic core and pointing forward (right; also see **Fig. 1b**, left). To probe the neck linker conformations in dimer in two-head-bound state, donor and acceptor fluorophores were attached to Cys215 and Cys342 in one polypeptide of a kinesin dimer (the second chain is Cys-light and is unreactive to dye labeling). (**b**) Histogram of FRET efficiencies of heterodimer kinesin with 215-342 dye pair in one of the heads bound to the axonemes in the presence of 1 mM AMP-PNP. Arrowheads illustrate two clear peaks in FRET efficiency. (**c**) Histograms of FRET efficiencies of G234A:E236A heterodimer kinesin bound to axonemes in the presence of 1 mM ATP. 215-342 dye pair was introduced into either G234A-containing polypeptide chain (upper) or E236A-containing chain (lower).

Distributions showed significant difference depending on which mutant chain is the recipient of the dyes pair (P value < 0.001 by Kolmogorov-Smirnov test). (**d**) Schematics of G234A:E236A heterodimer kinesin on the microtubule in the presence of ATP. G234A and E236A residues are shown in purple. The G234A head (neck linker is undocked, extending backwards) is predicted to be leading head, and the E236A head (neck linker is docked, extending forward) is predicted to be trailing. To test this idea, Cys in positions 43 and 215 were strategically introduced into the two mutant heads as shown. (**e**) Histograms of FRET efficiencies of G234A:E236A heterodimer kinesin bound to the axonemes in the presence of 1 mM ATP. 43 and 215 cysteines were introduced into G234A and E236A heads, respectively (upper), or into E236A and G234A heads, respectively (lower). Statistical test showed significant difference between these distributions (P value < 0.001).

Figure 3 Neck linker conformational changes in kinesin moving along microtubules under low ATP concentrations. (**a**) Four examples of time traces of fluorescence intensities of donor (Cy3; blue) and acceptor (Cy5; red) fluorophores, calculated FRET efficiency (E_{FRET}; green), and axial displacement of the centroid of fluorophores along axonemes (purple), of 215-342 heterodimer kinesin moving along axonemes in the presence of 0.5 or 1 μM ATP. Images were taken at 60 frames/sec and averaged over 4 frames. Black lines in fluorescence intensities and E_{FRET} traces show running-average over 7 frames. Black lines in the displacement traces are linear fits. Anti-correlated FRET changes (defined as anti-correlated transitions of >0.3 (see Methods)) are marked by vertical magenta dotted lines. Red arrows indicate the photobleaching of acceptor dye, and black arrows indicate the photobleaching of donor dye or detachment from the axoneme. (**b**) Relationship between the number of

transitions and the displacement of the motor; each point represents a different single molecule. Transitions were identified using traces after averaging as large FRET efficiency change (>0.3) that accompanies with clear anti-correlations (e.g. dotted vertical lines in panel **a**). Red line shows linear fit. (**c**) Example of time traces of fluorescence intensities, FRET efficiency, and axial displacement, for 43-215 heterodimer kinesin moving along axonemes in the presence of 1 μM ATP, showing little or no conformational changes of the catalytic core on this time scale. (**d**) Time traces of fluorescence intensities, FRET efficiency, and axial displacement, for 342:342 heterodimer kinesin moving along axonemes in the presence of 1 μM ATP, showing no unwinding of the coiled-coil. See **Supplementary Figures 3 and 5** online for additional single molecule traces. AU, arbitrary units.

Figure 4 A model, consistent with the FRET data, shows that the neck linkers switch between backwards extending (undocked) and forward extending (docked) conformational states during an 8 nm center-of-the mass displacement of the kinesin dimer (a 16 nm movement of the trailing head). See text for details as well as an alternative model involving a prolonged one-head bound intermediate during the dwell time between steps under low ATP concentration.

a

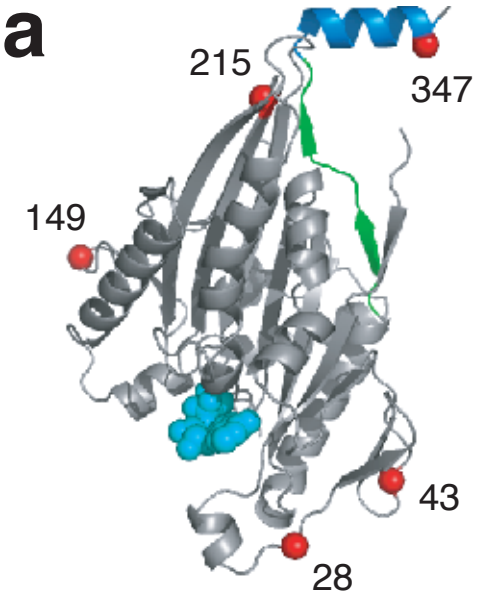

b

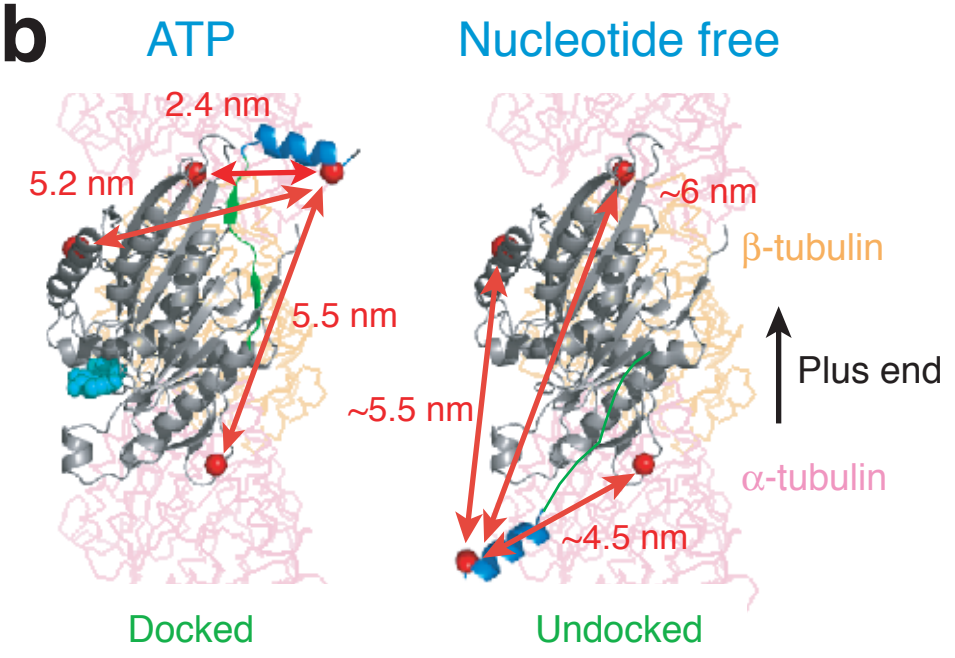

c

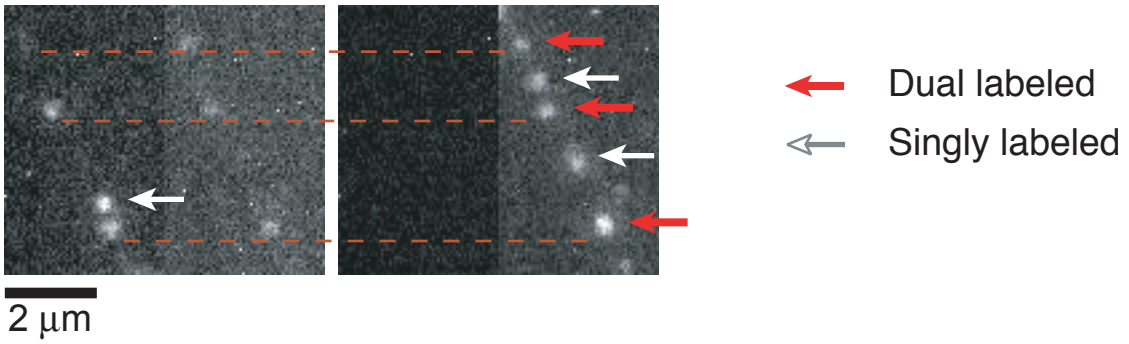

d

	FRET efficiency			
	215–347	43–347	149–347	28–149
AMP-PNP	0.79 ± 0.21 (50)	0.42 ± 0.18 (69)	0.51 ± 0.15 (39)	0.40 ± 0.16 (41)
Apyrase	0.28 ± 0.18 (44)	0.67 ± 0.22 (54)	0.47 ± 0.22 (33)	0.43 ± 0.12 (42)
E236A-ATP	0.81 ± 0.19 (61)	0.34 ± 0.11 (54)		
G234A-ATP	0.37 ± 0.18 (61)	0.81 ± 0.14 (61)		

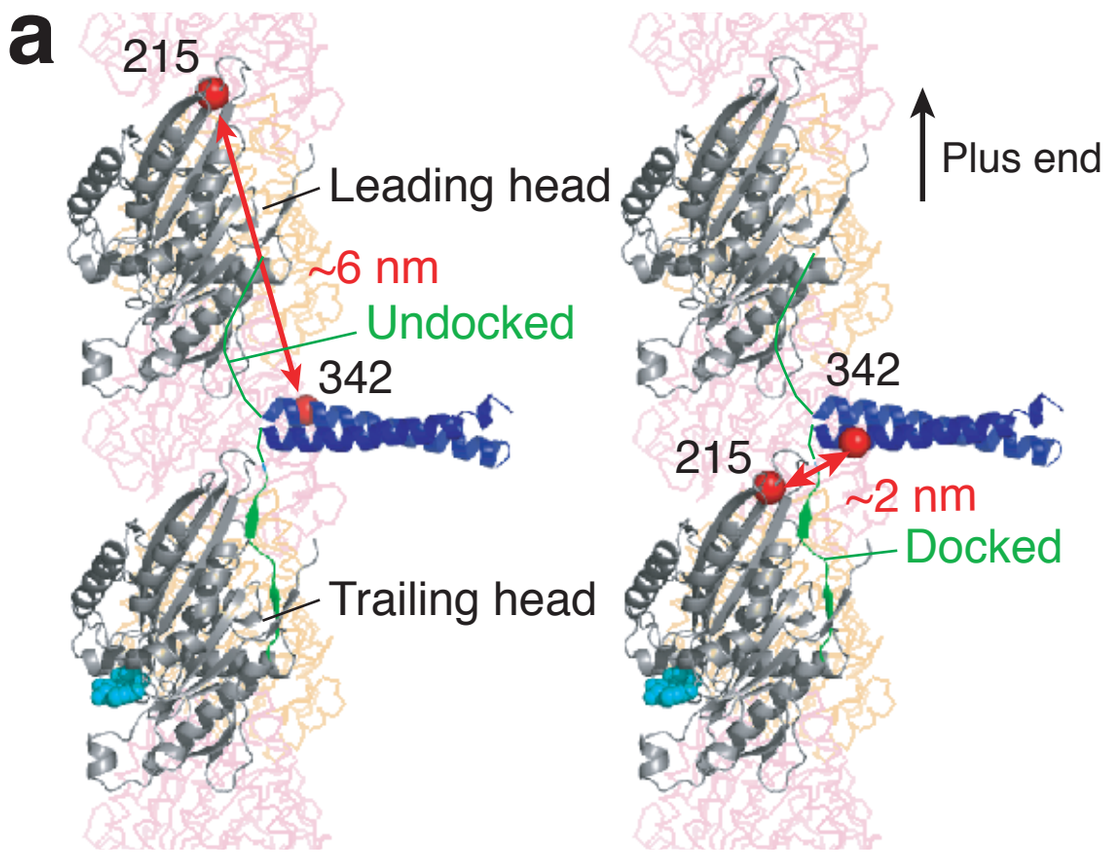
a
215
Leading head
~6 nm
Undocked
342
Trailing head
Plus end
342
215
~2 nm
Docked

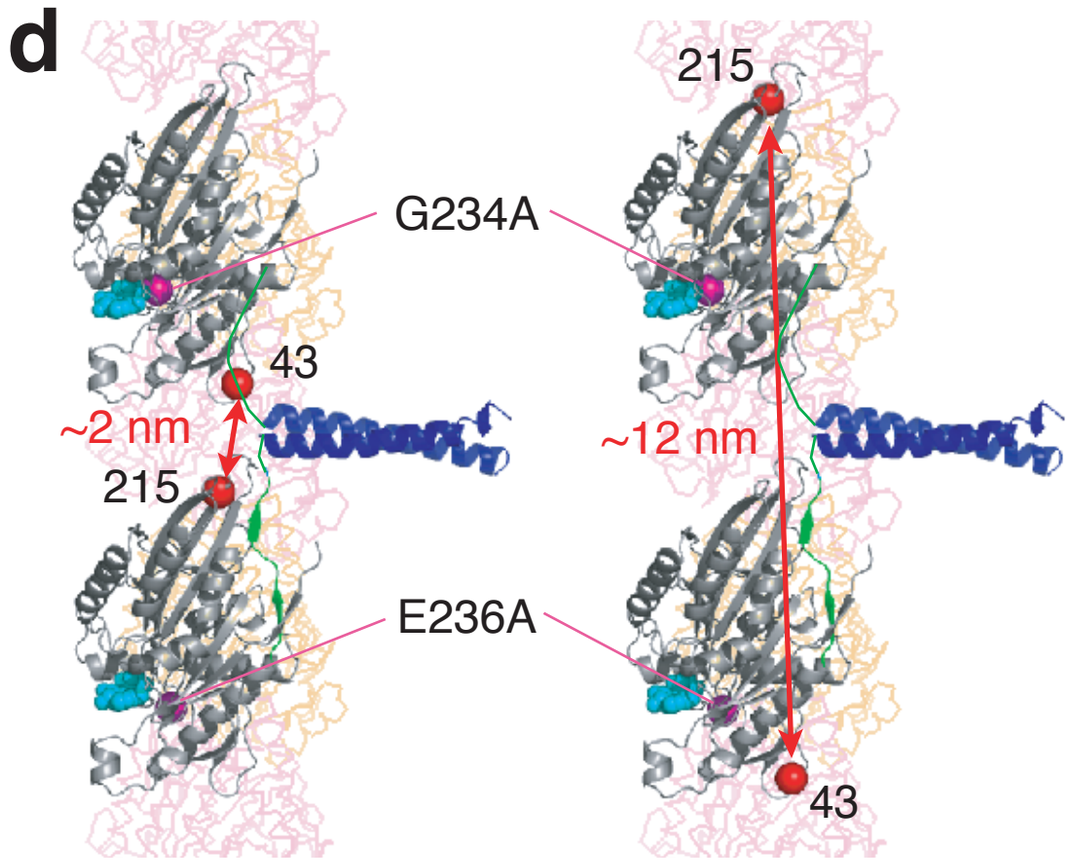
d
G234A
43
~2 nm
215
E236A
215
~12 nm
43

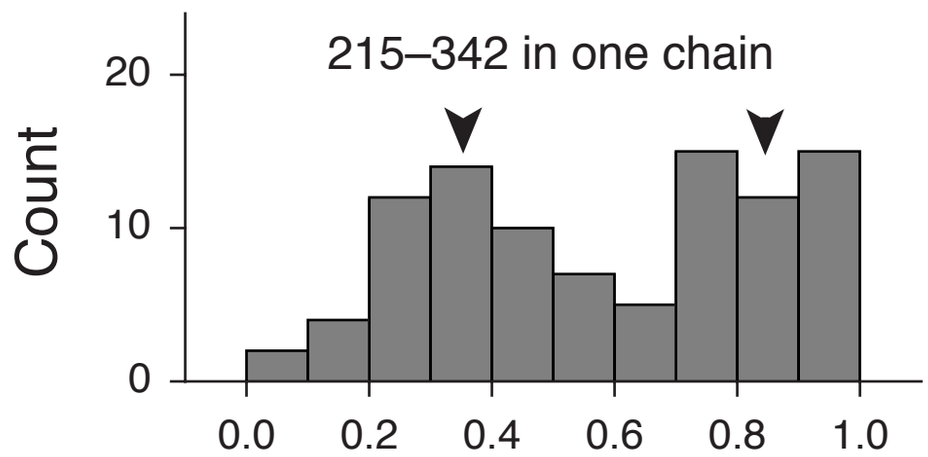
b
Wild type with AMP-PNP
215–342 in one chain
Count
20
10
0
0.0
0.2
0.4
0.6
0.8
1.0

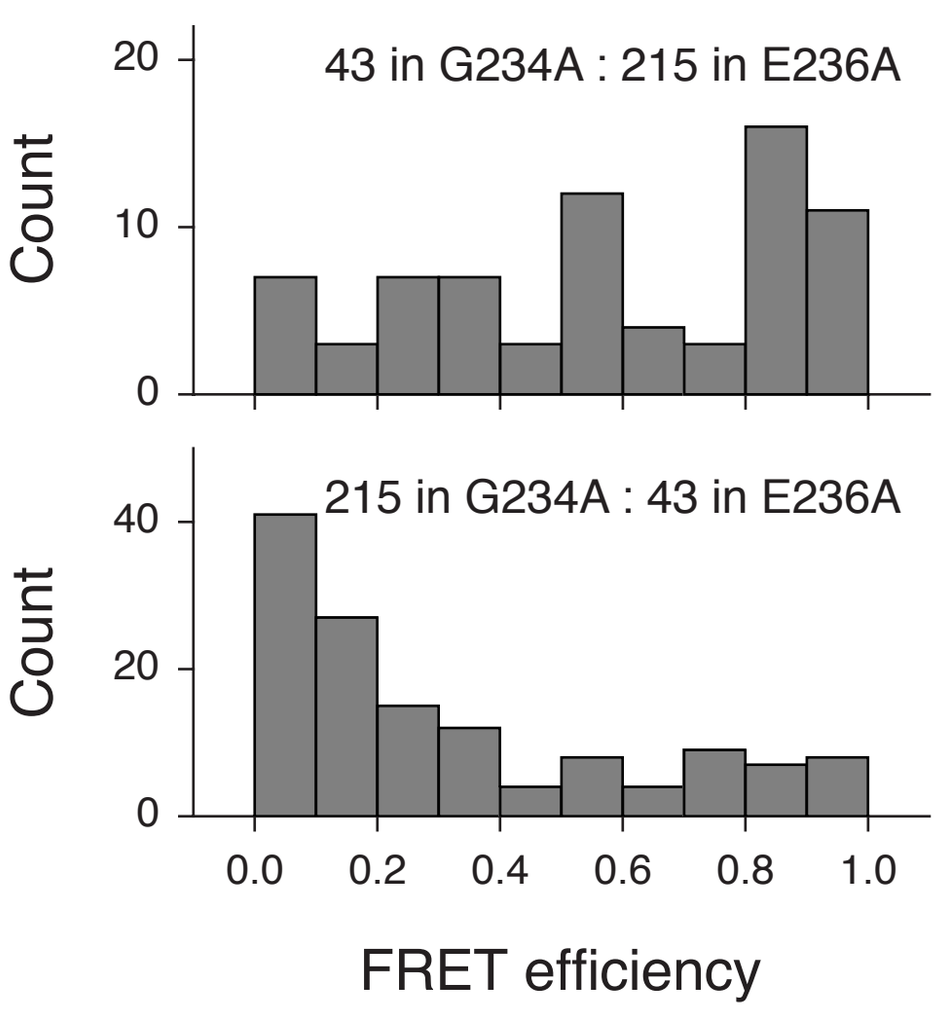
e
G234A : E236A heterodimer with ATP
43 in G234A : 215 in E236A
Count
20
10
0
215 in G234A : 43 in E236A
40
20
0
0.0
0.2
0.4
0.6
0.8
1.0
FRET efficiency

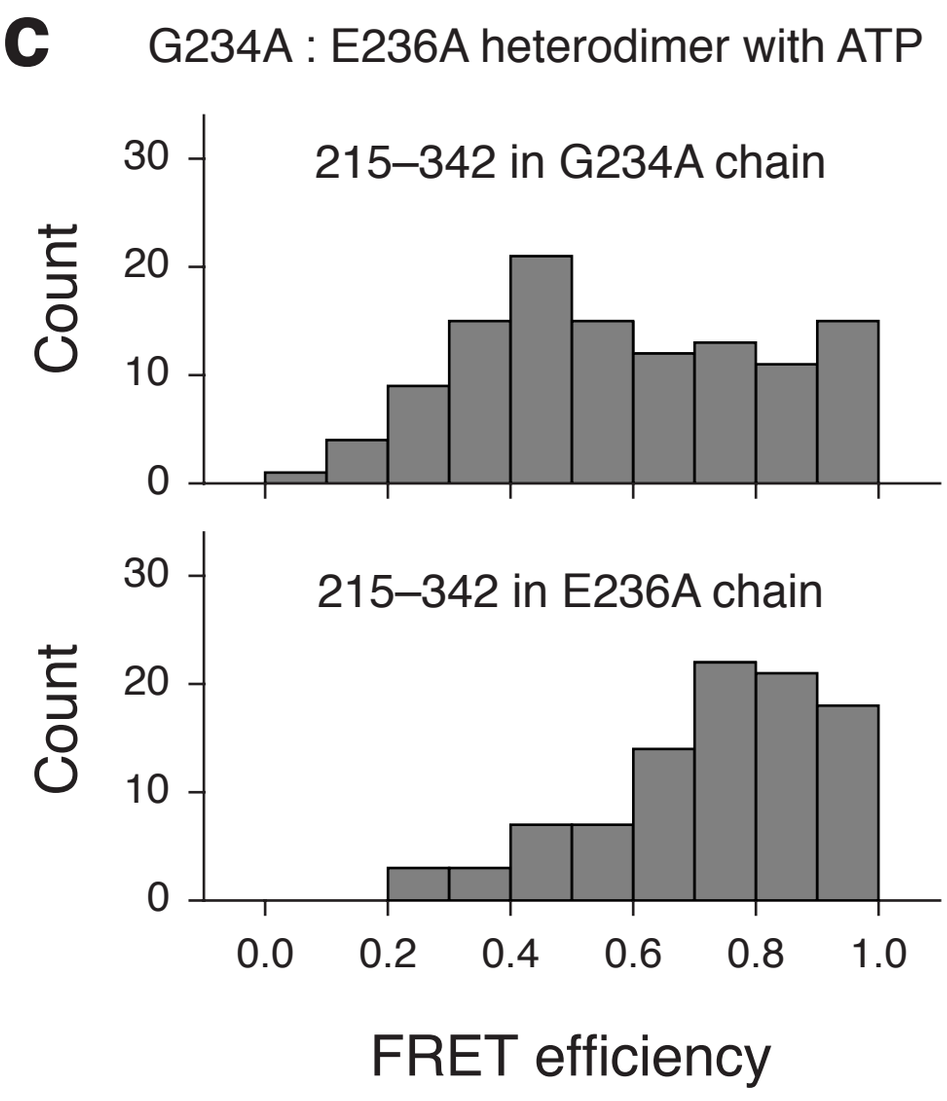
c
G234A : E236A heterodimer with ATP
215–342 in G234A chain
Count
30
20
10
0
215–342 in E236A chain
30
20
10
0
0.0
0.2
0.4
0.6
0.8
1.0
FRET efficiency

a

215–342 in one chain

Cy5

Cy3

Intensity (AU)

E_{FRET}

Displacement (nm)

Time (s)

b

16 nm per transition

11.2 nm per transition

8 nm per transition

Displacement (nm)

Number of transitions

c

43–215 in one chain

Intensity (AU)

E_{FRET}

Displacement (nm)

Time (s)

d

342 : 342

Intensity (AU)

E_{FRET}

Displacement (nm)

Time (s)

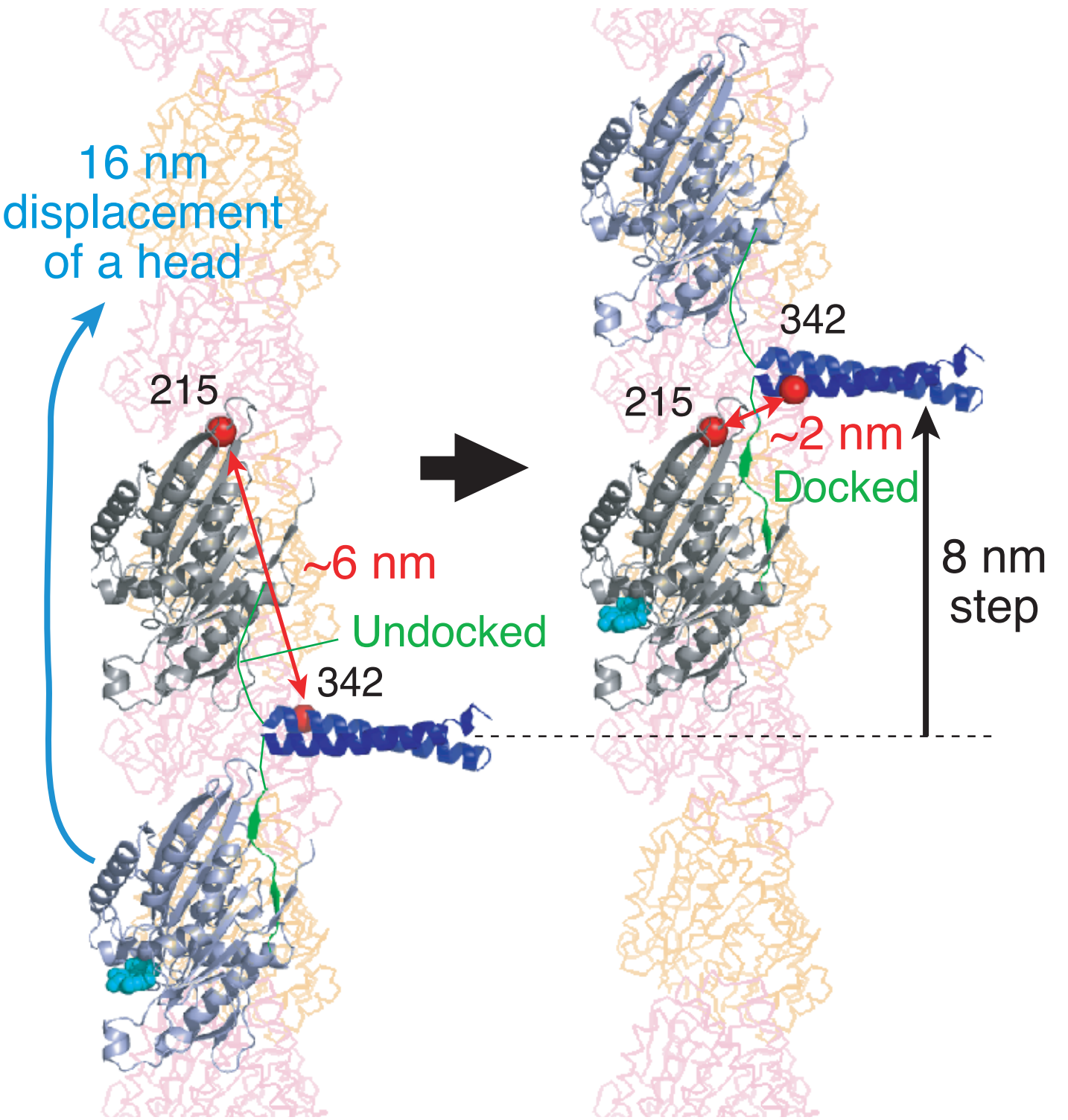
16 nm
displacement
of a head
215
342
~6 nm
Undocked
215
342
~2 nm
Docked
8 nm
step